BUTTERWORTH HEINEMANN

Polymer Vol. 36 No. 21, pp. 4069–4075, 1995

0032-3861/95/$10.00+0.00

Transverse isotropic elastic moduli and in-plane thermal diffusivity in silicon-supported thin films of a photosensitive polyimide measured using impulsive stimulated thermal scattering

Jennifer K. Cocson, Christine S. Hau, Peijou M. Lee, Clara C. Poon, Annita H. Zhong, John A. Rogers and Keith A. Nelson*

Department of Chemistry, Massachusetts Institute of Technology, Cambridge, MA 02139, USA

(Received 9 February 1995)

Through impulsive stimulated thermal scattering, the elastic and thermal properties of silicon-supported thin films (2–11 μm thicknesses) of a new low-CTE (coefficient of thermal expansion) photosensitive polyimide based on a biphenyl dianhydride/*p*-phenylenediamine backbone were studied. The material was found to be mechanically anisotropic. The in-plane thermal diffusivity and the in-plane and through-plane shear and longitudinal sound speeds were determined.

(Keywords: i.s.t.s. characterization; photosensitive thin film; elastic/thermal properties)

INTRODUCTION

Polymer thin films play crucial roles in a wide variety of industries such as microelectronics, automotive, paint and protective coatings, and biomedical. The ability to determine thermal and elastic properties of thin films in a rapid and non-invasive manner is crucial for assessment of film performance as well as for refinement of fabrication procedures. In a series of recent papers[1–6], a laser-based ultrasonic method known as impulsive stimulated thermal scattering (i.s.t.s.) has been introduced as a fast, non-invasive, non-contact, *in situ* means for evaluation of thin films. In this method, two laser pulses are spatially and temporally overlapped to create a sinusoidally varying 'grating' pattern on a film sample. Optical absorption at the grating peaks induces sudden ('impulsive') heating and thermal expansion in the sample with the same spatially periodic geometry. This gives rise to acoustic and thermal responses with a well defined wavevector magnitude q given by the wavelength λ_L of and the angle θ between the excitation pulses, i.e.

$$q = \frac{4\pi \sin(\theta/2)}{\lambda_L} = \frac{2\pi}{\Lambda} \quad (1)$$

where Λ is the grating fringe spacing. The acoustic and thermal responses result in time-dependent modulation ('ripple') of the film surface, and can be monitored through measurement of the intensity of time-dependent diffraction of a probe laser beam[2,7]. The acoustic response consists of counterpropagating ultrasonic waves, which give rise to damped oscillations in the diffraction intensity. The thermal response persists until thermal diffusion in or through the film plane returns the temperature gradient to zero between the grating peaks and nulls.

I.s.t.s. data from a single experiment at a selected wavevector magnitude q yield acoustic frequencies ω, velocities $v = \omega/q$ and damping rates, and the thermal diffusion rate at that wavevector. The mechanical properties, i.e. the elastic moduli (or equivalently, the shear and longitudinal acoustic velocities), and the in-plane thermal diffusivity of the film can be deduced from measurements at several wavevectors[1–3]. I.s.t.s. has been used for rapid and accurate non-invasive characterization of a variety of polymer films, including anisotropic films, as well as 'hard' coatings of various kinds[8]. Similar work has been done by Cachier[9] and Nakano and Nagai[10].

In this paper, we present the results of i.s.t.s. experimental characterization of the elastic and thermal properties of a recently developed[11] photosensitive polyimide (PSPI) based on biphenyl dianhydride (BPDA)/*p*-phenylenediamine (PPD). See *Scheme 1* for PSPI patterning photochemistry for the polyimide. The shear and longitudinal acoustic velocities and the thermal diffusivity of the photosensitive material are reported. The degree of anisotropy of the material is assessed and compared in molecular terms to that of the analogous non-photosensitive polymer film.

EXPERIMENTAL

The samples consisted of spin-coated and fully curved

* To whom correspondence should be addressed

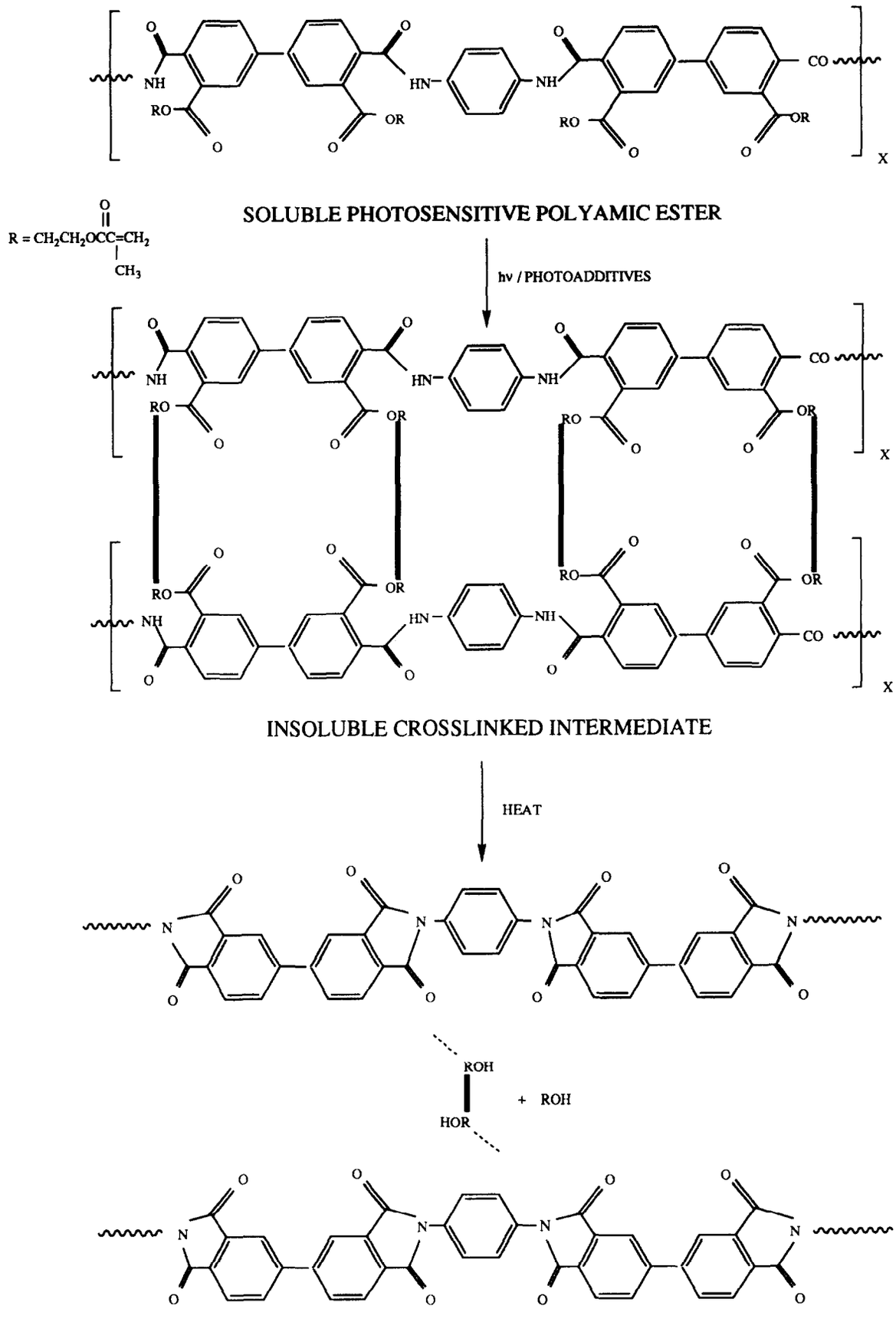

Scheme 1 PSPI patterning photochemistry

Table 1 The cure schedule for BPDA/PPD (DuPont 2734) thin films in air convection oven[11]

Prebake	55°C for 90 min
Irradiation	30 mJ cm^{-2} at 365 nm and 110 mJ cm^{-2} at 436 nm
Cure	150°C for 30 min
Bake	300°C for 30 min
Bake	400°C for 60 min

BPDA/PPD on 4 inch ($\sim$ 10 cm) diameter silicon wafers. After spinning, the coating was prebaked at 55°C for 90 min, crosslinked using u.v. irradiation, and fully cured in a convection oven under a schedule listed in *Table 1*[11]. The samples were fabricated at DuPont and have thicknesses of 2.95, 3.84, 5.61 and 10.66 ± 0.05 μm as measured with a mechanical stylus profilometer (Dektak 8000).

The i.s.t.s. experimental set-up is shown schematically in *Figure 1* and has been described in detail[2]. Briefly, the excitation pulses are derived from the frequency-doubled (532 nm) or frequency-tripled (355 nm) output of a Q-switched, mode-locked and cavity-dumped Nd:YAG laser. The probe beam is derived from a CW argon-ion laser (Coherent Innova 70-4, 1 W, single frequency, 514 nm) equipped with an electro-optic gate (Conoptics model 3) to yield a square pulse with an adjustable temporal width. The diffracted signal is monitored with a fast photodiode (Antel ARX-SA) and transient digitizing oscilloscope (Tektronix DSA 602A).

For the u.v. (355 nm) excitation pulses, the scattering angles θ used were 1.25, 1.35, 1.51, 1.75, 2.30, 2.69, 2.88, 3.23, 3.82 and 3.85 ± 0.05 degrees. Green (532 nm) excitation pulses were crossed at the following angles: 1.02, 1.70, 1.87, 2.11, 2.13, 2.39, 2.92 and 3.38 ± 0.05 degrees. The angles were measured using a mechanical rotation stage.

RESULTS

I.s.t.s. data: acoustic and thermal contributions

Figure 2 shows typical i.s.t.s. data from the 3.83 and 2.95 μm samples. The material response consists of damped acoustic oscillations on a nanosecond timescale followed by thermal diffusion on a microsecond time-scale. As the wavevector magnitude q varies with scattering angle, both the acoustic and thermal responses change. Thermal diffusion between grating peaks and nulls becomes faster as the grating period becomes smaller, i.e. at higher q. The acoustic response changes not only quantitatively, as discussed below in terms of acoustic frequencies and velocities, but qualitatively, in that the number and type of acoustic modes observed are wavevector-dependent. These changes are apparent in the acoustic data and power spectra shown in *Figure 2*. The q-dependent behaviour has been discussed in detail earlier[1,2] and will be described briefly here. When the film thickness d is comparable to or less than the acoustic wavelength Λ, i.e. $qd < 2\pi$, the film exhibits waveguide effects. In this regime, the acoustic response is no longer localized within the film, but extends into the substrate as well. Many acoustic waveguide modes, called pseudo-Rayleigh modes[12,13], propagate in the film–substrate system. Each mode has a distinct displacement pattern, which includes in-plane and out-of-plane longitudinal and shear components. The pseudo-Rayleigh acoustic velocities are therefore determined by both the in- and out-of-plane elastic properties of the film and the substrate. From i.s.t.s. measurements of the acoustic velocities at various wavevectors, the anisotropic elastic properties (i.e. in-plane and through-plane shear and longitudinal velocities) can be calculated.

In the limit that the film thickness is considerably less than the acoustic wavelength, the acoustic velocities approach those of the substrate. For a polymer film on a silicon substrate, the substrate effectively stiffens the system and the acoustic velocities increase as qd decreases. In the opposite limit of large qd, the acoustic wavelength is very short compared to the film thickness and the acoustic velocities are those of the bulk polymer material.

For most qd values, the lowest-order mode involves displacements largely confined to the free surface of the film. Strongly absorbed excitation pulses deposit most of their energy near this surface and thereby excite this mode efficiently. Higher-order modes involve displacements through the depth of the film. Weakly absorbed excitation pulses more efficiently couple to these modes. In the experiments described here, strongly absorbed u.v. (355 nm) and weakly absorbed visible (532 nm) excitation pulses were used in order to maximize the number of modes observed.

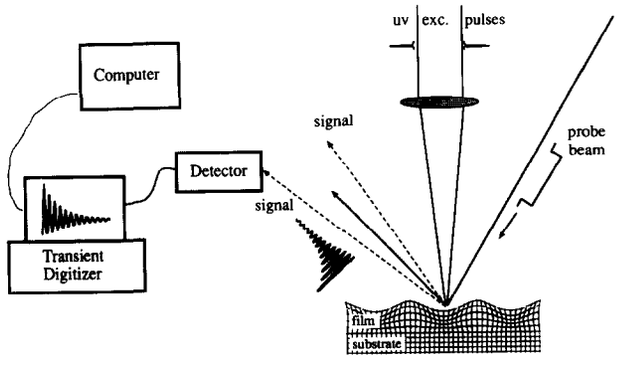

Figure 1 Experimental set-up for real-time i.s.t.s. experiments on supported thin films. Two excitation pulses are crossed at the film surface. Diffraction of a spatially and temporally overlapped probe laser beam is monitored, and the diffracted signal is time-resolved with a photodiode and a transient recorder

Acoustic signal and data analysis

Frequencies ω of the waveguide modes are obtained through Fourier transformation of the data and are used along with the values of q determined by equation (1) to determine the acoustic phase velocities. The q-dependent velocities of the two lowest-order modes are used in a non-linear least-squares fitting algorithm to determine shear and longitudinal velocities. In this fitting procedure, the film density and the substrate properties were fixed. We used values of 5341 and 8945 m s^{-1} for silicon shear and longitudinal velocities[14], respectively, and 2.33 g cm^{-3} for the density of silicon[15]. The value 1.5 g cm^{-3} was used as the density of the film[16]. We note that, although this density was measured using the non-photosensitive version of the polyimide film studied here, a change of this parameter by up to 20% has little effect on the best-fit velocities. The data from all

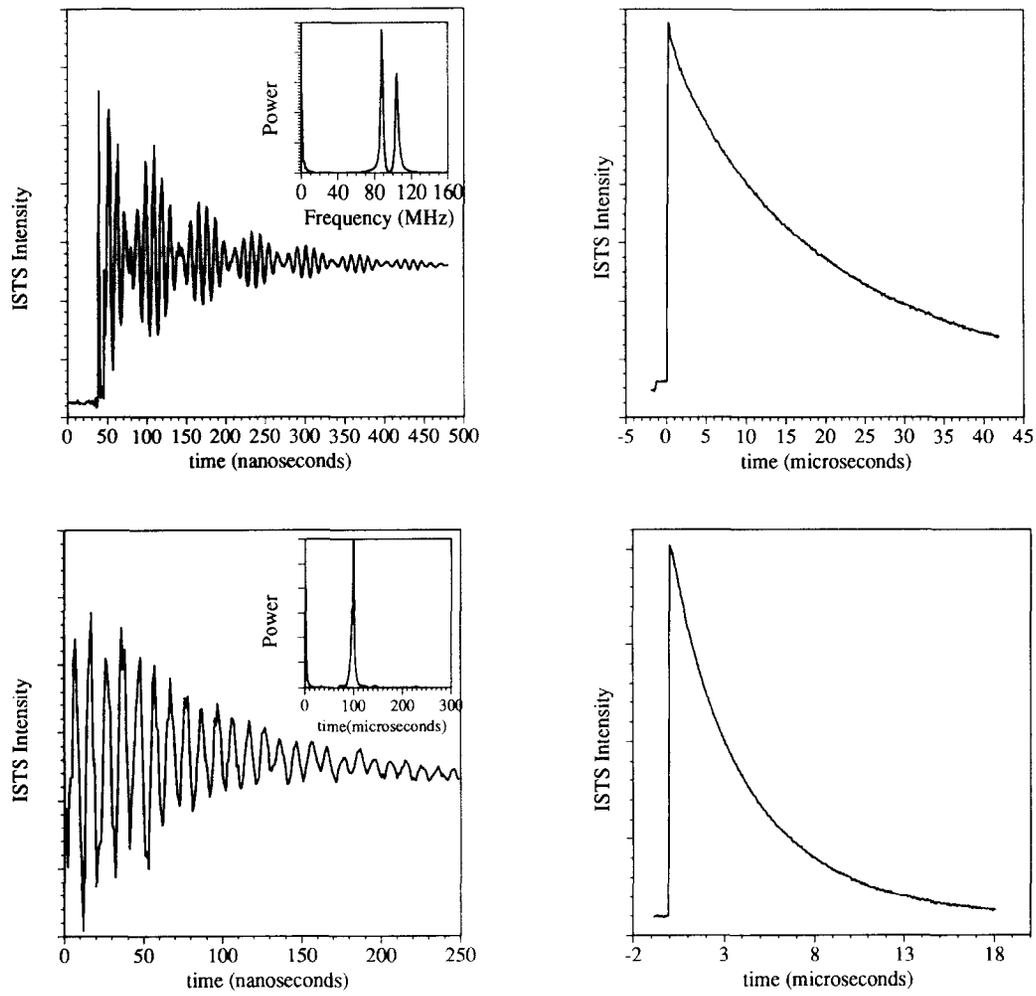

Figure 2 Diffracted i.s.t.s. signal from a 3.83 μm supported BPDA/PPD sample with an excitation wavelength of 532 nm (upper two frames) and from a 2.95 μm supported sample with an excitation wavelength of 355 nm (lower two frames). These data are the result of 200 averages and require several seconds to acquire. The two left frames show the damped acoustic oscillations on a nanosecond timescale, and the two right frames show the thermal diffusion on a microsecond timescale. In the upper 3.83 μm sample, where there is a beating pattern and two prominent peaks in the power spectrum, two Lamb modes were clearly excited

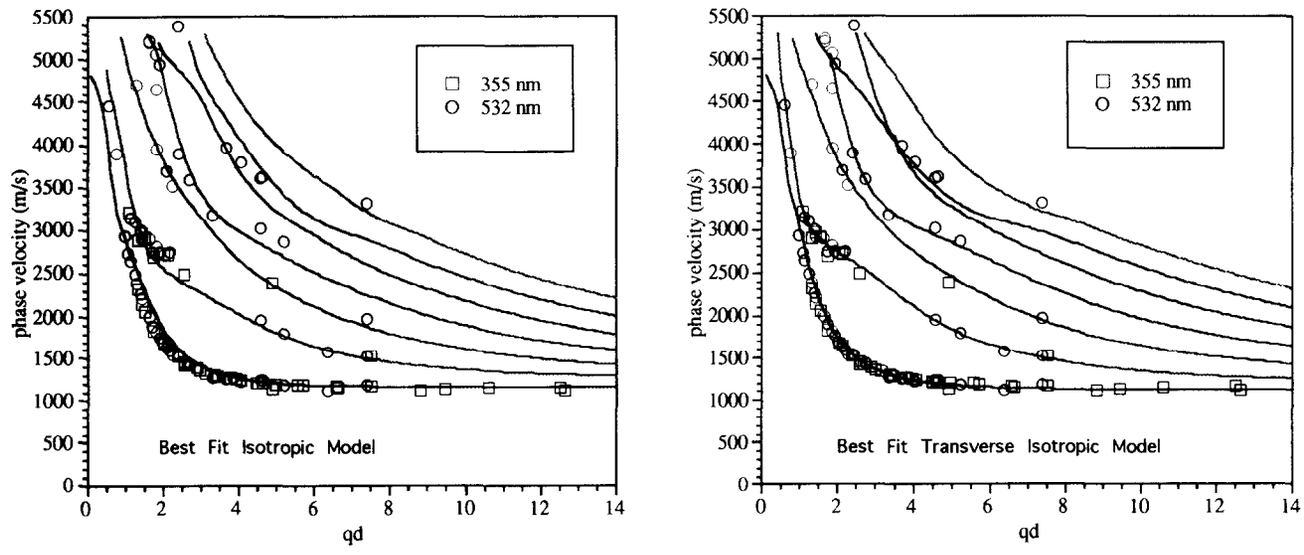

Figure 3 Acoustic dispersions of BPDA/PPD using (left) an isotropic model and (right) a transverse isotropic model. There are clear systematic inconsistencies in the lowest mode of the dispersion for the isotropic model. Measured data, however, agree well with the transverse isotropic mode

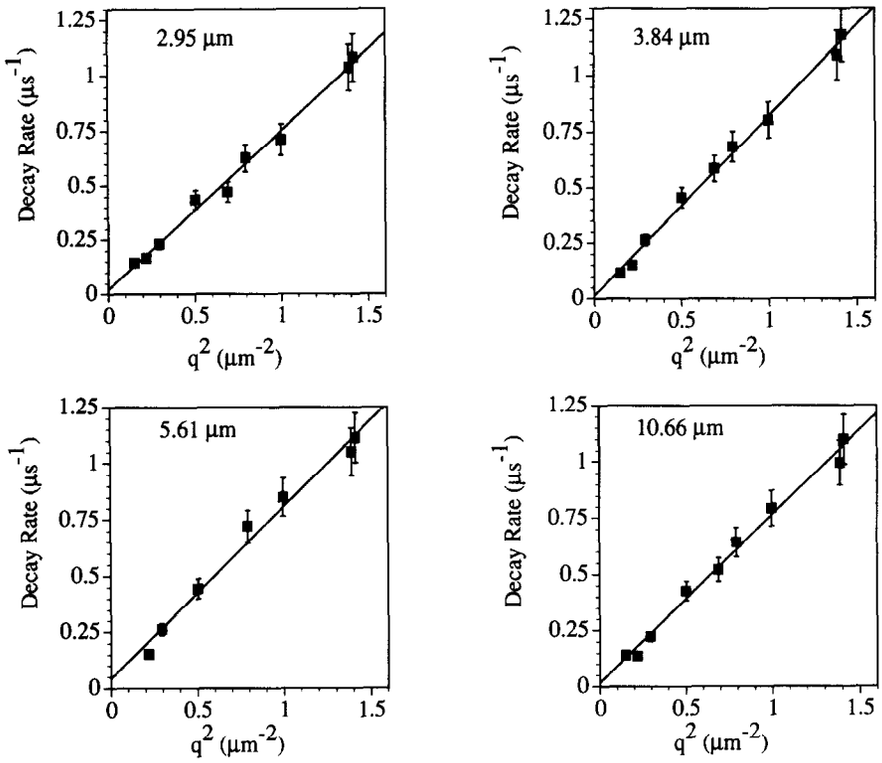

Figure 4 Thermal decay rate as a function of wavevector squared for four BPDA/PPD samples with various thicknesses (2–11 μm). The in-plane thermal diffusivities are determined by halving the slopes of the plots

samples were simultaneously fitted using both an isotropic model and a transverse isotropic model. (In the latter the in-plane properties are isotropic but are different from the out-of-plane properties.) Best fits based on each of these models along with data from all samples are displayed in *Figure 3*. It is apparent that the velocities measured at many q values from films of different thicknesses d scale with the qd product. This indicates that the elastic properties show no systematic thickness-dependence or sample to sample variation. For each of the models, higher-order modes were calculated using best-fit parameters determined from fitting the two lowest modes. As can be seen, the measured dispersion is reproduced well with the transverse isotropic model but not the isotropic model. Although the deviations of the data points from the isotropic fits appear small, they are systematic and well outside of experimental uncertainties. Based on this fact, we can conclude that the film mechanical properties are anisotropic. The average elastic properties of all samples are listed in *Table 2*.

Thermal signal and data analysis

Three factors govern the thermal decay rate: (1) the intrinsic in- and through-plane thermal diffusivities; (2) the scattering angle between the excitation pulses, which determines the magnitude of the wavevector and thus how far heat must travel in the in-plane direction to wash out the thermal grating; and (3) the nature of out-of-plane heat flow, e.g. the convection coefficient at the air–film interface and the thermal impedance between the film and the substrate. It has been shown that the time-dependent diffraction efficiency due to thermal decay is[17]:

$$\eta(t) = f^2(t)\exp(-2D_T q^2 t) \qquad (2)$$

where $f(t)$ describes out-of-plane heat flow and is dependent on quantities such as the out-of-plane thermal diffusivity, the excitation wavelength absorption depth, the convection coefficient at the air–film interface, and other material parameters associated with signal generation. The exponential term describes the in-plane thermal

Table 2 Summary of elastic and thermal properties determined by i.s.t.s. measurements of supported BPDA/PPD (DuPont 2734)

	Sample thickness (μm)			
Properties	2.95	3.84	5.61	10.66
In-plane shear velocity (m s^{-1})		1650 ± 200		
Out-of-plane shear velocity (m s^{-1})		1170 ± 100		
In-plane longitudinal velocity (m s^{-1})		3000 ± 300		
Out-of-plane longitudinal velocity (m s^{-1})		2350 ± 300		
In-plane thermal diffusivity (μm^2 μs^{-1})	0.37 ± 0.01	0.40 ± 0.01	0.38 ± 0.02	0.37 ± 0.01

Table 3 Mechanical and thermal properties of non-photosensitive BPDA/PDA films

Properties	Best fit values
In-plane longitudinal acoustic speed	$3580 \pm 150\,m\,s^{-1}$
In-plane shear acoustic speed	$2050 \pm 100\,m\,s^{-1}$
Out-of-plane longitudinal acoustic speed	$2330 \pm 100\,m\,s^{-1}$
Out-of-plane shear acoustic speed	$1130 + 50\,m\,s^{-1}$
In-plane thermal diffusivities	$0.60 \pm 0.01\,\mu m^2\,\mu s^{-1}$

Table 4 Residual stress values of the non-photosensitive (PI) and photosensitive (PSPI) polymer films (adapted from ref. 11)

	Stress (MPa)
PI IIIA	2.0
PSPI IIIB	42.2

flow, where D_T denotes the in-plane thermal diffusivity and q denotes the magnitude of the excitation wavevector as defined by equation (1). Typical measured thermal decays are illustrated in *Figure 2*.

At relatively large wavevector magnitudes, i.e. short peak–null distances, the decay is dominated by in-plane thermal diffusion. At these wavevectors, the second part of equation (2) decays completely before $f(t)$ undergoes any significant change. In this case the out-of-plane heat flow described by $f(t)$ can be described approximately as a single exponential, and the time-dependent decay of diffraction efficiency $\eta(t)$ becomes a single exponential as well. The thermal decay rates as determined from the slope of $\ln \eta(t)$ are then expected to show linear q^2-dependence. In this case, the in-plane thermal diffusivity is found by halving the slope of the plot of decay rates *versus* q^2. The y intercept is related to the out-of-plane thermal flow rate. *Figure 4* shows such plots for the four BPDA/PPD samples analysed. In calculating in-plane thermal diffusivities, data measured at the smallest wavevectors in which the decays were non-exponential were discarded. Also not included in the calculation are data recorded with green excitation pulses. Because of their larger absorption length, the green pulses may deposit heat onto the substrate as well as in the film and increase the importance of film–substrate heat exchange. The in-plane thermal diffusivities of the four sample films, ranging from 0.37 to $0.40\,\mu m^2\,\mu s^{-1}$ (see *Table 2*), are found to be consistent with one another within the uncertainty range. The results indicate that the in-plane thermal diffusivity of the BPDA/PPD polyimide thin film is thickness-independent over the thickness range ($2-11\,\mu m$) investigated.

The y intercepts of the decay rate plots vs. q^2 are related to the out-of-plane thermal flow rates. However, owing to the small values and large percentage uncertainties in the y intercepts, no useful information regarding out-of-plane thermal flow can be obtained. The randomness in y intercepts *versus* thickness, nevertheless, indicates that there is not significant film-to-substrate heat flow.

Finally, we note that the thermal decay rates showed significant ($\pm 10\%$) spot-to-spot variations within a single film, which were comparable to the variations (20%) between films at large q values. The spot-to-spot variations are outside the range of uncertainties in the measurements, and therefore reflect genuine variation within the films.

DISCUSSION

It is interesting to note that the elastic and thermal properties of the photosensitive BPDA/PPD differ significantly from those of the non-photosensitive BPDA/PPD, which were studied in detail previously (see *Tables 2* and *3*)[4,16]. In particular, the mechanical properties of the non-photosensitive BPDA/PPD are more anisotropic and the in-plane thermal diffusivity is much larger than those of the photosensitive BPDA/PPD. We speculate that the differences between the

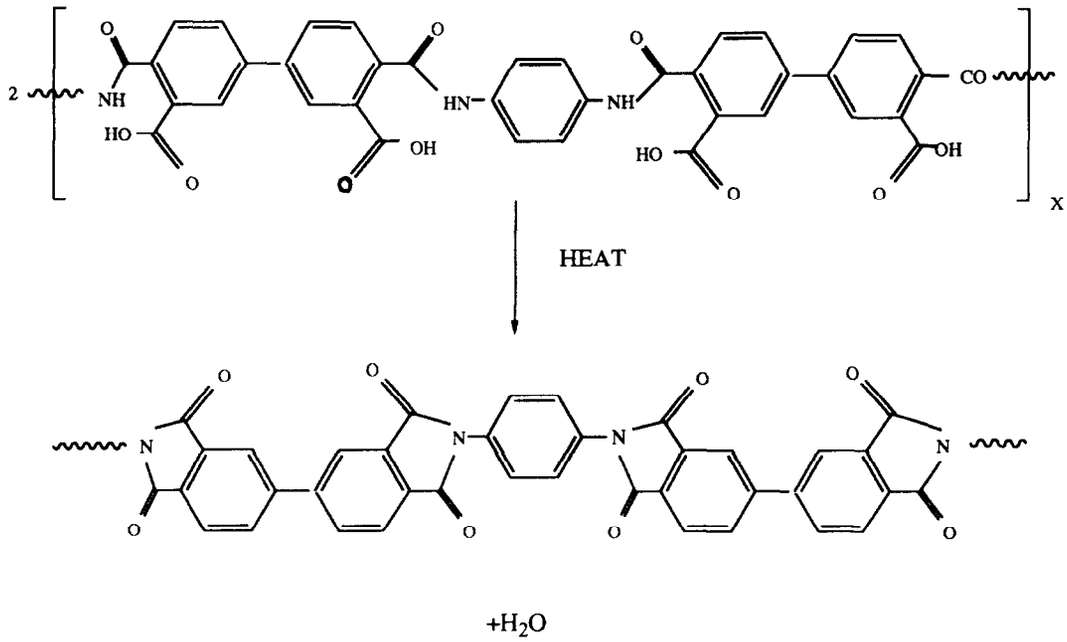

Scheme 2 PI chemistry

chemical structures of the two polymer precursors are the cause of this result. These differences are apparent in *Schemes 1* and *2*. The BPDA/PPD polymer precursor is made photosensitive through replacement of carboxyl hydrogen atoms with bulky 2-hydroxyethyl methacrylate (HEMA) photosensitizers (denoted as R groups) to form the photosensitive poly(amic ester). The bulky R groups may frustrate in-plane chain orientation by forcing the polymer chain to bend so as to minimize steric interactions between the R groups. In contrast, the small H atoms could permit in-plane chain orientation by allowing the chain to lie flat in the plane. This difference in orientation could be at least partially maintained throughout the curing step, and for the photosensitive polyimide could give rise to a decreased number of covalent bonds in the film's plane and an increased number of covalent bonds out of the film's plane. Because of this, we would expect the in-plane mechanical properties, e.g. shear and longitudinal velocities, to decrease and the out-of-plane mechanical properties to increase. The in-plane thermal diffusivity of the photosensitive BPDA/PPD could also decrease, because the heat flows less continuously in this direction. These trends were all observed in the data. The same conclusions were reached using X-ray and optical birefringence measurements on a similar photosensitive polyimide[18]. Furthermore, we note (see *Table 4*, ref. 11) that there is a significant increase in residual stress in the photosensitive BPDA/PPD (IIIB) thin films compared to the non-photosensitive BPDA/PPD (IIIA). This can also be explained by the difference in the degree of orientation in the polymer precursors.

CONCLUSIONS

Elastic and thermal properties of silicon-supported thin films of a recently developed HEMA-induced photosensitive biphenyl dianhydride (BPDA)/*p*-phenylenediamine (PPD) of thicknesses 2–11 μm were determined through i.s.t.s. A tranverse isotropic model was needed to describe accurately the observed elastic behaviour. In-plane shear and longitudinal velocities were determined to be 1650 ± 200 and $3000 \pm 300\,\mathrm{m\,s^{-1}}$, respectively, while out-of-plane shear and longitudinal velocities were determined to be 1170 ± 100 and $2350 \pm 300\,\mathrm{m\,s^{-1}}$, respectively. The in-plane thermal diffusivity typically falls within the range of $0.37–0.40\,\mu\mathrm{m^2\,\mu s^{-1}}$. For the thickness range investigated, it was found that the elastic and thermal properties are thickness-independent.

The lower degree of anisotropy and the lower in-plane thermal diffusivity in the photosensitive polymer relative to a non-photosensitive analogue were rationalized in terms of molecular structures, which would suggest a higher degree of in-plane orientation in the latter.

ACKNOWLEDGEMENTS

This work was supported in part by NSF Grant No. CHE-8951738, which provided initial equipment for an undergraduate picosecond laser spectroscopy laboratory, NSF Grant No. DMR-9317198, and the Donors of the Petroleum Research Fund, administered by the American Chemical Society. We wish to acknowledge full or partial donations of equipment from Tektronix, Coherent Laser, Con-Optics, Antel and Neslab. We thank Dr Wesley Schindel and Mr Mel Zussman at DuPont for providing samples.

REFERENCES

1 Duggal, A. R., Rogers, J. A. and Nelson, K. A. *J. Appl. Phys.* 1992, **60**, 692
2 Rogers, J. A. and Nelson, K. A. *J. Appl. Phys.* 1994, **75**, 1534
3 Rogers, J. A., Yang, Y. and Nelson, K. A. *Appl. Phys. (A) Solids Surf.* 1994, **58**, 523
4 Rogers, J. A., Dhar, L. and Nelson, K. A. *Appl. Phys. Lett.* 1994, **65**, 312
5 Rogers, J. A. and Nelson, K. A. *J. Adhes.* 1995, **50**, 1
6 Rogers, J. A., Mindas, C., Yang, Y. and Nelson, K. A. *Mater. Res. Soc. Symp. Proc.* 1993, **323**, 425
7 Rogers, J. A. and Nelson K. A. 'Ultrafast Pulse Generation and Spectroscopy', Proceedings of the Society of Photo-Optical Instrumentation Engineers Conference OE-LASE, 1993, Vol. 1861, pp. 314–25
8 Yang, Y., Nelson, K. A. and Adibi, F. *J. Mater. Res.* 1995, **10**, 41
9 Cachier, G, *Appl. Phys. Lett.* 1970, **17**, 419
10 Nakano, H. and Nagai, S. *Ultrasonics* 1991, **29**, 230
11 Nader, A. E., Imai, K., Craig, J. D., Lazaridis, C. N., Murray, D. O., III, Pottiger, M. T. and Lauternberger, W. J. in press
12 Auld, B. A. 'Acoustic Fields and Waves in Solids', Wiley, New York, 1973, Vol. 2
13 Viktorov, I. 'Rayleigh and Lamb Waves, Physical Theory and Applications', Plenum, New York, 1967
14 Anderson, O. L. in 'Physical Acoustics, Principles and Methods' (Eds. P. Mason and R. N. Thurston), Academic Press, New York, 1965, Vol. 3B, p. 77
15 Weast, R. C., Astle, M. J. and Beyer, W. H. (Eds), 'CRC Handbook of Chemistry and Physics', 64th Edn, CRC, Boca Raton, FL, 1983
16 Nenov, K. personal communication
17 Rogers, J. A. and Nelson, K. A. 'Materials Reliability in Microelectronics IV', Proceedings of the Spring 1994 Materials Research Society Meeting, Symposium C (Eds P. Borgesen, J. E. Sanchez Jr, J. C. Coburn, K. Rodbell and W. Filter), Vol. 338, pp. 553–63 (Note that the actual thermal diffusivities should be twice the reported values in this paper)
18 Ree, M. and Nunes, T. L. *Polymer* 1994, **35**, 1148